Available online at www.sciencedirect.com
SCIENCE DIRECT®
International Journal of Multiphase Flow 31 (2005) 723–738
International Journal of Multiphase Flow
www.elsevier.com/locate/ijmulflow

Modeling of droplet collision-induced breakup process

Gwon Hyun Ko, Hong Sun Ryou *

School of Mechanical Engineering, Chung-Ang University, Seoul, Korea

Received 20 July 2004; received in revised form 9 February 2005

Abstract

The present article proposes a new droplet collision model considering droplet collision-induced breakup process with the formation of satellite droplets. The new model consists of several equations to investigate the post-collision characteristics of colliding droplets and satellite droplets. These equations are derived from the conservations of droplet mass, momentum, and energy between before and after collision, and make it possible to predict the number of satellite droplets, and the droplet size and velocity in the analytical way. To validate the new collision model, numerical calculations are performed and their results are compared with experimental data published earlier for binary collision of water droplets. It is found from the results that the new model shows good agreement with experimental data for the number of satellite droplets. It can be also shown that the predicted mean diameter by the new model decrease with increasing the Weber number because of the collision-induced breakup, whereas the O'Rourke model fails to predict the size reduction via the binary droplet collision.

Keywords: Collision-induced breakup; Coalescence; Separation; Satellite droplet

1. Introduction

Collision dynamics of liquid droplets is important in evolution of sprays used in various industrial applications, e.g., commercial furnace, internal combustion engines, surface treatment

* Corresponding author. Tel.: +82 2 820 5280; fax: +82 2 816 4972.
E-mail address: cfdmec@cau.ac.kr (H.S. Ryou).

0301-9322/$ - see front matter © 2005 Elsevier Ltd. All rights reserved.
doi:10.1016/j.ijmultiphaseflow.2005.02.004

process, water mist system for fire suppression, and so forth. In dense spray system (O'Rourke and Bracco, 1980) and interspray impingement system (Arai and Saito, 1999; Ko et al., 2003), droplet collision can significantly affect the spray characteristics, such as drop size and velocity distribution. It is thus important to investigate the droplet collision characteristics and to develop the relevant numerical model for collision process.

Generally, the post-characteristics of droplet collisions are described by three non-dimensional parameters as follows (Ashgriz and Poo, 1990; Orme, 1997; Post and Abraham, 2002):

$$We = \rho D_1 |\vec{u}_{\mathrm{rel}}|^2 / \sigma, \tag{1}$$

$$\Delta = D_1 / D_2, \tag{2}$$

$$b = 2B/(D_1 + D_2), \tag{3}$$

where We is the Weber number based on droplet diameter, Δ the droplet size ratio, and b is the impact parameter. ρ and σ are the density and the surface tension of liquid phase, and the subscripts 1 and 2 represent smaller and larger droplets, respectively. B is calculated by taking the distance from the center of one droplet to the relative velocity vector, $\vec{u}_{\mathrm{rel}}$, placed on the center of the other droplets, as illustrated in Fig. 1. The outcomes from collision are classified four different types: bounce, coalescence, reflexive separation, and stretching separation, as seen in Fig. 2. As two droplets impinge each other, the gas between them is trapped and the pressure increases inside this gap. If relative velocity of droplets is not enough to overcome the pressure force, two droplets do not impinge and go away from each other. This is referred to as bounce. For higher relative velocity, on the other hand, one droplet contacts another directly and in turn coalescence process takes place between them. At high Weber numbers, the droplets have excess kinetic energy, which leads to the separation of droplets from droplet coalesced tentatively. The temporarily coalesced droplets tend to undergo a reflexive separation and a stretching separation at low and high impact parameters, respectively. Many researchers (Ashgriz and Poo, 1990; Qian and Law,

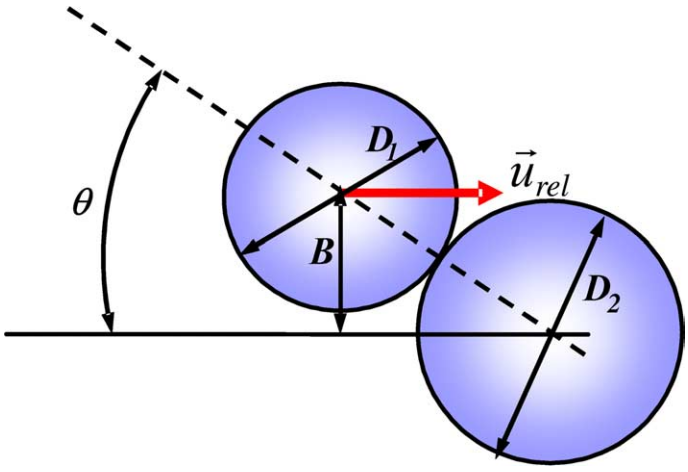

Fig. 1. Kinetic and geometric parameters of the droplet collision.

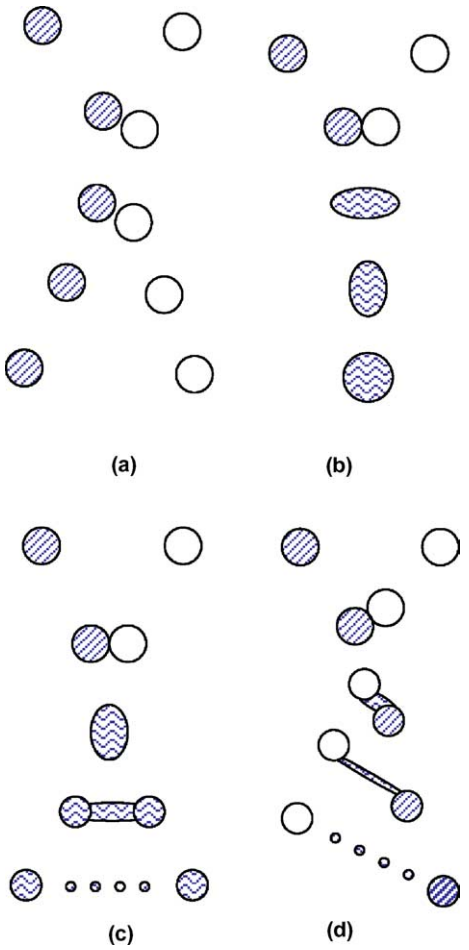

Fig. 2. Diagram of collision regimes: (a) bouncing; (b) coalescence; (c) reflexive separation; (d) stretching separation.

1997) observed that the separations produce the satellite droplets from the interacting parts between two colliding droplets, and in turn results in the size reduction in droplets. This procedure is called a collision-induced breakup process whose effects are more pronounced as Weber number increases.

In most of numerical simulation on spray dynamics, the model of O'Rourke (1981) has been commonly used for the droplet collision process. O'Rourke (1981) derived the equation about the collision probability using the classical kinetic theory on the basis of the assumption that the droplets were uniformly distributed inside the sprays and the droplet collision had similarity to the molecular collision process. He also modeled the post-characteristics of droplets using the balance equations of mass, velocity, and energy between before and after collision. However, there are some problems that the O'Rourke model includes only coalescence and grazing separation. It means that the O'Rourke model cannot mimic other important processes related to the binary collision, e.g., reflexive and stretching separations, and corresponding formation of satellite droplets. According to results of Ko et al. (2003), the O'Rourke model substantially overpredicted

the droplet size and failed to predict the overall spray shapes appearing in the interspray impingement system, where two solid cone sprays are directly impinged at the prescribed position and droplets collides each other with high relative velocities.

The main purposes of the present study are thus in development of the new model for the droplet collision-induced breakup process. For clarifying the post-characteristics for separation collisions, mass, momentum, and energy conservation equations are derived in an appropriate way during the collision procedure. From these equations, such important formulae are obtained for the number of the satellite droplets, and the sizes and velocities of droplets. For assessment of the new model, the comparisons of numerical predictions with experimental data (Ashgriz and Poo, 1990; Brenn et al., 2001) are additionally conducted for post-characteristics of binary droplet collision process.

2. The O'Rourke model

The present study develops the new droplet collision model including the breakup process induced by droplet collision, and the new model is compared with the O'Rourke model which has been widely utilized in the numerical works on the spray behaviors. This section at first introduces the O'Rourke's model briefly, and then the new model of droplet collision will be derived and its physical meanings will be also discussed in next section.

Among outcomes of droplet collision, the O'Rourke model considers three regimes of bounce, permanent coalescence, and separation, but ignores the formation of the satellite droplets. Fig. 3 shows the boundaries between the regimes adopted in the O'Rourke model for the collision of equal-sized droplets. Followings explain the relationships in O'Rourke model for the criteria and the post-collision characteristics of three regimes. The transition criterion from coalescence to separation is given in terms of coalescence collision efficiency E_{coal} as follows (Brazier-Smith et al., 1972):

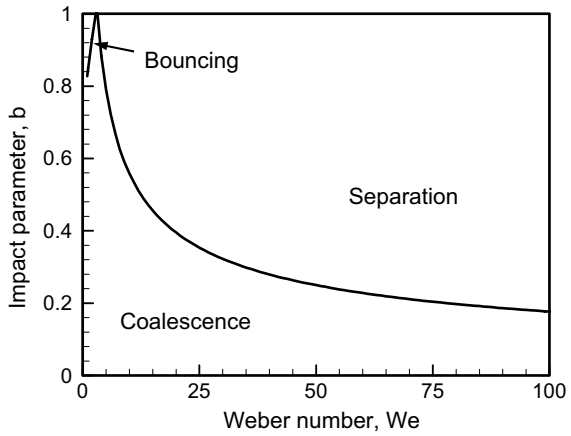

Fig. 3. Boundaries between collision regimes adopted in the O'Rourke (1981) model for $\Delta = 1$.

$$E_{\text{coal}} = \min\left[1, \frac{2.4f(\gamma)}{We_s}\right], \tag{4}$$

where $f(\gamma) = \gamma^3 - 2.4\gamma^2 + 2.7\gamma$, $\gamma = D_2/D_1$, and $We_s = \rho \mid \vec{u}_{\text{rel}}|^2(D_1 + D_2)/2\sigma$. In addition, the subscripts 1 and 2 represent smaller and larger droplets, respectively. The regime boundary between coalescence and separation is therefore determined by $b = E_{\text{coal}}$. In other words, coalescence occurs if impact parameter b is less than E_{coal} and otherwise the separation occurs. Brazier-Smith et al. (1972) observed the grazing bouncing when the equal-sized water drops collide at low relative velocity. They suggested a critical Weber number We_s of 2.12 below which grazing is only possible and a critical collision parameter, E_{boun}, above which grazing bouncing is only possible. The O'Rourke model determines E_{boun} by

$$E_{\text{boun}} = \min\left[1, \left(\frac{We_s}{2.4f(\gamma)}\right)^{1/3}\right]. \tag{5}$$

The grazing bounce collision thus takes place when $We_s < 2.12$ and $b > E_{\text{boun}}$.

The post-collision properties of the collision regimes such as droplet diameters and velocities are determined from the conservation equations of mass, linear momentum, and angular momentum (O'Rourke, 1981). In coalescence regime, the droplet mass and the velocity are expressed as

$$D_{1a} = \left(\frac{\rho_1 D_1^3 + n\rho_2 D_2^3}{\rho_{1a}}\right)^{1/3}, \tag{6}$$

$$\vec{u}_{1a} = \frac{\left(\rho_1 D_1^3 \vec{u}_1 + n\rho_2 D_2^3 \vec{u}_2\right)}{\rho_{1a} d_{1a}^3}, \tag{7}$$

where the subscript a denotes a value after collision and n is the number of coalescence. In the separation and grazing bounce regimes, no mass is assumed to exchange between two colliding droplet parcels. The velocities are determined as

$$\vec{u}_{1a} = \frac{\rho_1 D_1^3 \vec{u}_1 + \rho_2 D_2^3 \vec{u}_2 + \rho_2 D_2^3 (\vec{u}_1 - \vec{u}_2)\left(\frac{b-\sqrt{E}}{1-\sqrt{E}}\right)}{\rho_1 D_1^3 + \rho_2 D_2^3}, \tag{8}$$

$$\vec{u}_{2a} = \frac{\rho_1 D_1^3 \vec{u}_1 + \rho_2 D_2^3 \vec{u}_2 + \rho_2 D_2^3 (\vec{u}_2 - \vec{u}_1)\left(\frac{b-\sqrt{E}}{1-\sqrt{E}}\right)}{\rho_1 D_1^3 + \rho_2 D_2^3}, \tag{9}$$

where E represents the critical collision efficiencies of Eqs. (4) and (5) for the separation and the grazing bounce regimes, respectively. For more details, good summary is well documented in references (O'Rourke and Bracco, 1980; O'Rourke, 1981; Bai, 1996).

3. New droplet collision model

As mentioned previously, the O'Rourke model considers only three collision regimes such as separation, permanent coalescence, and grazing bounce. Moreover, even in separation regime,

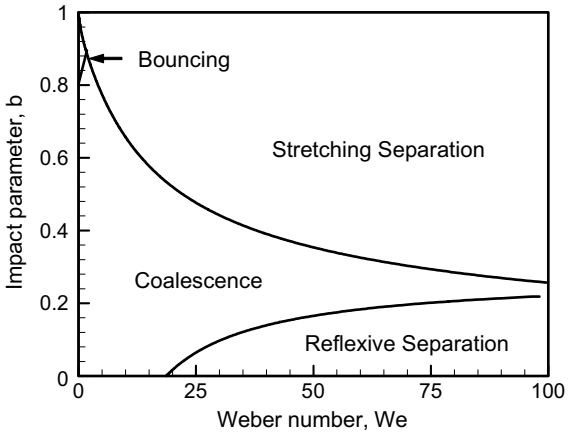

Fig. 4. Boundaries between collision regimes adopted in the new model for $\Delta = 1$.

the colliding droplets lose only their momentum, but retain their sizes after impact. As referred by Bai (1996), the O'Rourke model could overpredict the coalescence phenomenon because the collision-induced breakup processes are ignored. Ashgriz and Poo (1990) divided the separation processes into two classes of the stretching separation and the reflexive separation. Many other researchers (Qian and Law, 1997; Estrade et al., 1999; Brenn et al., 2001) also showed that the satellite droplets are formed in the processes and the size of droplet decreases after collision correspondingly. Above all, it is necessary to consider the collision-induced breakup process for simulating the interspray impingement system more precisely (Ko et al., 2003).

In the present study, the model for stretching and reflexive separation processes is newly derived to consider the collision-induced breakup including the satellite droplet formation phenomena. Fig. 4 shows the boundaries between regimes adopted in the present model for the binary collision of equal-sized droplets. Stretching and reflexive separations take place when two colliding droplets satisfy Eq. (13) and Eq. (37), respectively. Otherwise, one of bounce and coalescence processes occurs and the post-characteristics of collision are calculated using the O'Rourke model. In what follows, the mathematical relationships are introduced for the post-collision characteristics of stretching and reflexive separation processes.

3.1. Stretching separation

At the beginning, the present study discusses the mechanism of stretching separation from Ashgriz and Poo (1990)'s theory. When two droplets collide at the high impact parameter, only a portion of them will come in direct contact as seen in Fig. 5. Ashgriz and Poo (1990) calculated the interaction region (the hatched parts in Fig. 4) of two colliding droplets as follows:

$$V_{ji} = \phi_j V_j, \tag{10}$$

$$\phi_1 = \begin{cases} 1 - \frac{1}{4\Delta^3}(2\Delta - \lambda)^2(\Delta + \lambda) & \text{for } h > \frac{D_1}{2}, \\ \frac{\lambda^2}{4\Delta^3}(3\Delta - \lambda) & \text{for } h < \frac{D_1}{2}, \end{cases} \tag{11}$$

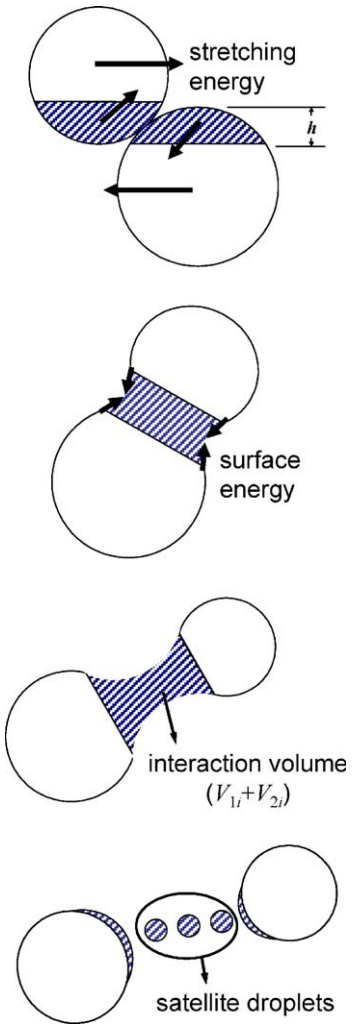

Fig. 5. Schematic of the stretching separation collision of two droplets.

$$\phi_2 = \begin{cases} 1 - \frac{1}{4}(2-\lambda)^2(1+\lambda) & \text{for } h > \frac{D_2}{2}, \\ \frac{\lambda^2}{4}(3-\lambda) & \text{for } h < \frac{D_2}{2}, \end{cases} \tag{12}$$

where $\lambda \equiv (1-b)(1+\Delta)$ and the interaction height, $h = 0.5(D_1 + D_2)(1-b)$. Additionally, V is the volume of droplet, Δ the size ratio of two droplets, b the impact parameter, subscript i is the interaction portion of droplets, and subscript $j = 1, 2$. They assumed that the stretching separation would occur when the effective stretching energy KE_{st} exceeded the surface tension energy SE_i of the interaction region. They expressed this condition by the following equations:

$$KE_{\mathrm{st}} \gg SE_i, \tag{13}$$

$$KE_{\mathrm{st}} = \frac{1}{2}\rho\left[(V_1 - V_{1i})\vec{u}_1^2 + (V_2 - V_{2i})\vec{u}_2^2 + V_{1i}(\vec{u}_1 b)^2 + V_{2i}(\vec{u}_2 b)^2\right], \tag{14}$$

$$SE_i = 2\sigma[\pi h(\phi_1 V_1 + \phi_2 V_2)]^{1/2}, \tag{15}$$

where $\vec{u}_1$ and $\vec{u}_2$ are the velocities of the smaller and larger droplets in the mass-centre coordinates, respectively, as given by $\vec{u}_1 = \vec{u}_{\mathrm{rel}}/(1+\Delta^3)$ and $\vec{u}_2 = -\Delta^3\vec{u}_{\mathrm{rel}}/(1+\Delta^3)$, where $\vec{u}_{\mathrm{rel}}$ is the relative velocity of two droplets. The above equations showed good agreements with experimental data for the regime boundary between stretching separation and coalescence. However, Ashgriz and Poo (1990) did not offer any empirical or theoretical relationship on the droplet velocity and size, essential for describing the stretching separation numerically.

It is necessary to determine the separating volume from the colliding two droplets in order to define the post-collision characteristics of droplets. From the visualization data reported by Ashgriz and Poo (1990) and Qian and Law (1997), it is found that during the stretching separation process, a portion of the interaction volume only forms the satellite droplets and the rest returns to the original colliding droplets. This process is represented in Fig. 5. Thus, the separating volume becomes smaller than the interaction volume. In order to take account for these phenomena, the present model defines the separation volume coefficient on the assumption that the separating volume is proportional to the ratio of the energy required for separation to the total energy of two droplets. The separation volume coefficient of stretching collision is defined by

$$C_{VS} = \frac{KE_{\mathrm{st}} - SE_i}{KE_{\mathrm{st}} + SE_i}. \tag{16}$$

Using the above equation, the separating volume and the size of colliding droplets after collision are calculated as follows:

$$V_{\mathrm{s}} = C_{VS}(V_{1i} + V_{2i}), \tag{17}$$

$$D_{ja} = (1 - C_{VS}\phi_j)^{1/3} D_j, \tag{18}$$

where subscript s means the separation portion and $j = 1, 2$. For simplicity, all satellite droplets are assumed to have same properties, and then the mass and momentum conservation equations are can be written as

$$D_1^3 + D_2^3 = D_{1a}^3 + D_{2a}^3 + N_{\mathrm{sa}} \cdot D_{\mathrm{sa}}^3, \tag{19}$$

$$D_1^3\vec{u}_1 + D_2^3\vec{u}_2 = D_{1a}^3\vec{u}_1 + D_{2a}^3\vec{u}_2 + N_{\mathrm{sa}} \cdot D_{\mathrm{sa}}^3\vec{u}_{\mathrm{sa}}, \tag{20}$$

where N_{sa} is the number of satellite droplets. If the reminder of colliding droplets is assumed to retain their velocity, i.e.,

$$\vec{u}_{ja} = \vec{u}_j, \tag{21}$$

where subscript $j = 1, 2$. The diameter and velocity of satellite droplets are derived from Eqs. (19) and (20) as follows:

$$D_{\mathrm{sa}} = \left[\frac{C_{VS}(\phi_1\Delta^3 + \phi_2)}{N_{\mathrm{sa}}}\right]^{1/3} D_2, \tag{22}$$

$$\vec{u}_{\mathrm{sa}} = \frac{\Delta^3(\phi_1 - \phi_2)}{(1+\Delta^3)(\Delta^3\phi_1 + \phi_2)}\vec{u}_{\mathrm{rel}}. \tag{23}$$

In order to determine the number of satellite droplets, the excess surface energy must be calculated, which redistributes the separation volume into the satellite droplets. The energy conservation between before and after impact is represented as follows:

$$KE_1 + SE_1 + KE_2 + SE_2 = KE_{1a} + SE_{1a} + KE_{2a} + SE_{2a} + KE_{\mathrm{s}} + SE_{\mathrm{s}} + DE, \tag{24}$$

where KE, SE, and DE represent the kinetic, surface tension, and dissipation energies, respectively. The kinetic and surface energies of colliding droplets after collision are calculated as follows:

$$KE_{ja} = \frac{1}{2}\rho V_{ja}\vec{u}_{ja}^2, \tag{25}$$

$$SE_{ja} = \rho\pi D_{ja}^2, \tag{26}$$

where subscript $j = 1, 2$. The total kinetic energy of satellite droplets can be represented by

$$KE_{\mathrm{s}} = N_{\mathrm{sa}} \cdot \left(\frac{1}{2}\rho\frac{\pi}{6}D_{\mathrm{sa}}^3\right)u_{\mathrm{sa}}^2 = \frac{1}{2}\rho V_{\mathrm{s}}\vec{u}_{\mathrm{sa}}^2. \tag{27}$$

The dissipation energy DE can be in general defined as follows:

$$DE = \int\int \mu\left(\frac{\partial u_i}{\partial x_j} + \frac{\partial u_j}{\partial x_i}\right)^2 \mathrm{d}V\,\mathrm{d}t. \tag{28}$$

Using the relationship suggested by Jiang et al. (1992) who expressed the viscous dissipation in terms of the kinetic energy of interaction volume, the following equation is introduced for the dissipation energy:

$$DE = \alpha\left(\frac{1}{2}\rho(V_{1i}\vec{u}_1^2 + V_{2i}\vec{u}_2^2)\right), \tag{29}$$

where α denotes the energy loss coefficient. For water droplets, α has been empirically determined to be around 0.5 by Jiang et al. (1992). Then, the total surface tension energy SE_{s} of the satellite droplets can be calculated from Eq. (24), and the number of satellite droplets is determined using Eq. (22) as follows:

$$N_{\mathrm{sa}} = \left[\frac{SE_{\mathrm{s}}}{\sigma\pi C_{VS}^{2/3}(\Delta^3\phi_1 + \phi_2)^{2/3}D_2^2}\right]^3. \tag{30}$$

Now, the post-characteristics of the stretching separation can be calculated using Eqs. (18), (21)–(23), and (30).

3.2. Reflexive separation

The reflexive separation takes places for the head-on or near-centre collisions of two droplets and the schematic of this process is shown in Fig. 6. Ashgriz and Poo (1990) explained this process

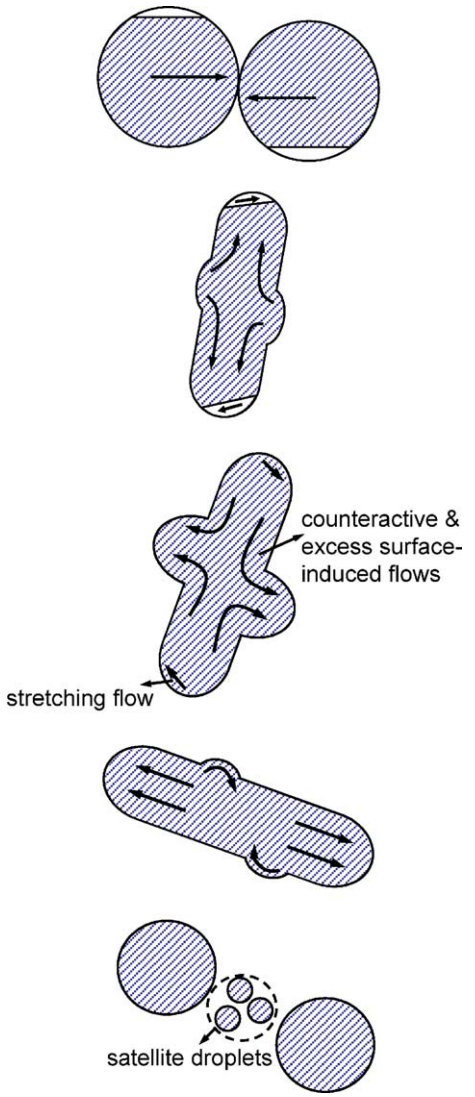

Fig. 6. Schematic of reflexive separation for the off-centre collision of two droplets.

using the balance between the effective reflexive energy and the surface energy of the temporarily coalesced droplet. According to their theory, the effective reflexive energy KE_{er} consists of the kinetic energies of counteractive flows, excess surface-induced flows, and stretching flows as follows:

$$KE_{er} = KE_{co} + KE_{es} - KE_{st}, \tag{31}$$

$$KE_{co} = \frac{1}{2}\rho\left(V_{1i}\vec{u}_1^2 + V_{2i}\vec{u}_2^2\right), \tag{32}$$

$$KE_{es} = \sigma\pi d_2^2\left[(1+\Delta^2) - (1+\Delta^3)^{2/3}\right], \tag{33}$$

$$KE_{st} = \frac{1}{2}\rho\left[(V_1 - V_{1i})\vec{u}_1^2 - (V_2 - V_{2i})\vec{u}_2^2\right], \tag{34}$$

where subscripts co, es and st mean the counteractive, excess surface-induced, and stretching flows, respectively. As seen in above equations, Ashgriz and Poo (1990) assumed that the stretching flows reduce the reflexive energy. Additionally, the interaction volume (the shadow region of the first figure in Fig. 6) of reflexive separation process is determined by

$$V_{1i} = \frac{1}{6}\pi D_2^3(\Delta - \xi)^2(\Delta^2 - \xi^2), \tag{35}$$

$$V_{2i} = \frac{1}{6}\pi D_2^3(1 - \xi)^2(1 - \xi^2), \tag{36}$$

where $\xi = 0.5b(1 + \Delta)$. They postulated that reflexive separation will occur when the effective reflexive kinetic energy is more than 75% of the surface energy of nominal spherical droplets coalesced temporarily. The value of 75% was introduced to consider the deformation effect of the nominal droplets. Thus, the criterion for reflexive separation is

$$KE_{er} \geqslant SE_{nd}, \tag{37}$$

$$SE_{nd} = 0.75\sigma\pi(D_1^3 + D_2^3)^{2/3}. \tag{38}$$

On the basis of Ashgriz and Poo (1990)'s theory, the present study newly derives the mathematical formulations for the post-collision characteristics in the reflexive separation, will be referred below. Similar to the stretching collision process, the reflexive separation process accompanies with the formation of satellite droplet (Ashgriz and Poo, 1990; Qian and Law, 1997). In order to determine the volume separated from the colliding droplets, the present study thus introduces the new parameter C_{VR}, called the separation volume coefficient that is defined as the ratio of separating volume to total volume of two colliding droplets. It is assumed here that this coefficient C_{VR} is proportional to the ratio of energy required for separation to energy of two colliding droplets as follows:

$$C_{VR} = \frac{KE_{er} - SE_{nd}}{KE_{er} + SE_{nd}}. \tag{39}$$

Thus, the separating volume and the new diameter of the colliding droplets are determined by

$$V_s = C_{VR}(V_1 + V_2), \tag{40}$$

$$D_{ja} = (1 - C_{VR})^{1/3}D_j, \tag{41}$$

where subscript $j = 1, 2$. For liquid volume separated from two colliding droplets, the mass and momentum equations are represented by

$$C_{VR}D_1^3 + C_{VR}D_2^3 = N_{sa}D_{sa}^3, \tag{42}$$

$$C_{VR}D_1^3\vec{u}_1 + C_{VR}D_2^3\vec{u}_2 = C_{VR}(D_1^3 + D_2^3)\vec{u}_{sa}. \tag{43}$$

Correspondingly, the size and velocity of satellite droplets are given from the mass conservation law as follows:

$$D_{\mathrm{sa}} = \left[\frac{C_{VR}}{N_{\mathrm{sa}}}\left(D_1^3 + D_2^3\right)\right]^{1/3}, \tag{44}$$

$$\vec{u}_{\mathrm{sa}} = \frac{D_1^3\vec{u}_1 + D_2^3\vec{u}_2}{D_1^3 + D_2^3}. \tag{45}$$

In determining the number of satellite droplets, the surface energy of separating volume should be calculated. The energy conservation can be written as follows:

$$KE_1 + SE_1 + KE_2 + SE_2 = KE_{1a} + SE_{1a} + KE_{2a} + SE_{2a} + KE_{\mathrm{s}} + SE_{\mathrm{s}} + DE. \tag{46}$$

Contrary to the stretching separation, because the viscous dissipation will occur in the nominal droplet, the dissipation energy DE is proportional to the total kinetic energy of the colliding droplets as follows:

$$DE = \alpha\left(\frac{1}{2}\rho\left(V_1\vec{u}_1^2 + V_2\vec{u}_2^2\right)\right). \tag{47}$$

Considering this energy loss, the kinetic energy and the velocity of colliding droplets can be written as

$$KE_{ja} = \frac{1}{2}\rho V_{ja}\vec{u}_{ja}^2, \tag{48}$$

$$\vec{u}_{ja} = (1-\alpha)^{1/2}\vec{u}_j, \tag{49}$$

where subscript $j = 1, 2$. Additionally, the surface energy of colliding droplets after collision is given by

$$SE_{ja} = \rho\pi D_{ja}^2. \tag{50}$$

Thus, the surface energy of separating volume SE_{s} is determined from Eq. (46), and then the number of satellite droplets is calculated from Eq. (44) as follows:

$$N_{\mathrm{sa}} = \left[\frac{SE_{\mathrm{s}}}{\sigma\pi C_{VR}^{2/3}\left(D_1^3 + D_2^3\right)^{2/3}}\right]^3. \tag{51}$$

The post-characteristics of the reflexive separation are finally determined by Eqs. (41), (44), (45), (49), and (51).

4. Results and discussion

This section examines the predictability of new model by comparing the predicted results with earlier published experimental data (Ashgriz and Poo, 1990; Brenn et al., 2001) for the binary collision of two droplets. Fig. 7 shows the predicted *We-b* maps for the number of satellite droplets in

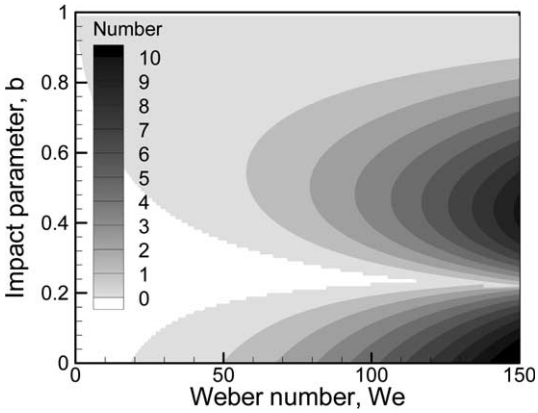

Fig. 7. Calculated number distribution of satellite droplets for binary collision of two water droplets for $\Delta = 1$.

case that the binary collision of two equal-sized water droplets takes place. In this calculation, the energy loss coefficient α is 0.5 suggested by Jiang et al. (1992). In the stretching separation regime, the number of satellite droplets is of the highest value in the range from 0.4 to 0.6 in impact parameter. Until the impact parameter reaches to 0.4, the number of satellite droplets increases because of the increase in the stretching energy. When the impact parameter ranges from 0.6 to 1.0, on the other hand, the probability of satellite droplet formation is reduced due to the decrease in interaction region between two colliding droplets. In the reflexive separation regime, in addition, the satellite droplets are formed most actively in the case of the head-on collision. As mentioned previously, it can be supported by the fact that the stretching effects induced by off-centre collision reduce the reflexive separation.

Fig. 8 compares the predicted *We*-*b* map only for the stretching collision of equal-sized propanol-2 droplets with the experimental data of Brenn et al. (2001). Compared to Fig. 7, it is found that the number of satellite droplets for propanol-2 droplets is smaller than that of water droplets.

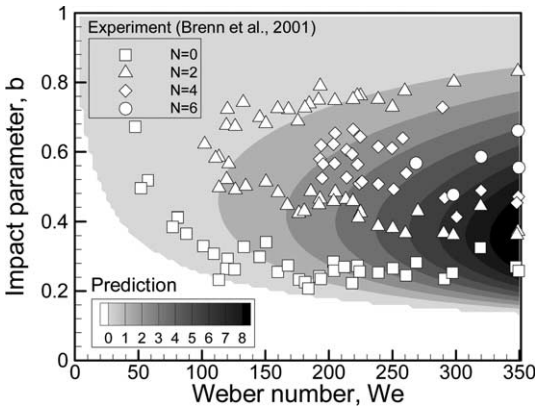

Fig. 8. Comparison of the calculated number distribution of satellite droplets with experimental data (Brenn et al., 2001) for stretching separation collision of equal-sized propanol-2 droplets.

According to the Orme (1997), the droplet collision phenomena highly rely upon the droplet property. By the contrast in the collision of water droplets, the bouncing phenomena occur over the wide range of Weber number, and also the surface tension energy loss becomes more significant in the collision of fuel droplets. For this reason, the formation of satellite droplets due to the stretching separation is relatively suppressed in the collision of the propanol-2 droplets. In this figure, the present model slightly underestimates the regime criterion between coalescence and stretching separation regimes, and the impact parameters where the highest number of droplets occurs. This is because the present model does not consider the loss of surface tension energy and the bouncing collision over the wide range of *We*. Nevertheless, the predictions of present model agree well with the experimental data qualitatively in the distribution of satellite droplet numbers.

In Figs. 9 and 10, comparisons are made between the predictions and the experimental data of Ashgriz and Poo (1990) for the number of satellite droplets. As seen in Figs. 9 and 10, the present model predicts well compared to the experimental data for the stretching separation and for the head-on collision at different conditions. For the head-on collision, it is found that the number of satellite droplets increase with the Weber number.

In Fig. 11, the normalized mean diameter is presented for different Weber numbers and it is averaged over the whole range of impact parameter at a given Weber number. Here, D_{10} and SMD denote the arithmetic and Sauter mean diameters, respectively. They are often used to analyze the characteristics of droplet size distributions in applications of liquid spray. Over the range of low Weber number, both models predict the increase of mean diameter after collisions because of droplet coalescence. As the Weber number increases, however, both D_{10} and SMD computed by the new model decrease gradually, indicating that the droplet breakup via collision increases with Weber number. Since the O'Rourke model ignores the reflexive separation process at low impact parameters as well as the change in droplet size even in stretching separation process, the predictions of the O'Rourke model are rarely varied over the whole range of Weber number. From

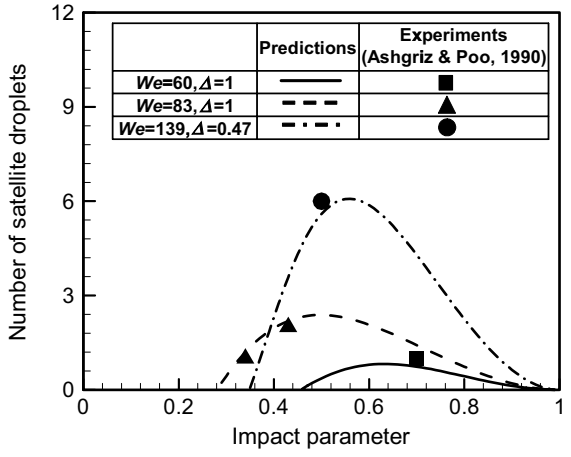

Fig. 9. Comparison of the calculated satellite droplet number with experimental data (Ashgriz and Poo, 1990) for stretching separation collision of two water droplets.

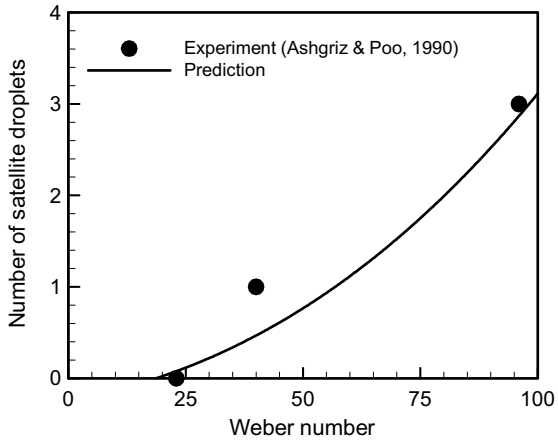

Fig. 10. Comparison of the calculated satellite droplets number with the experimental data (Ashgriz and Poo, 1990) for the head-on collision of two equal-sized water droplets.

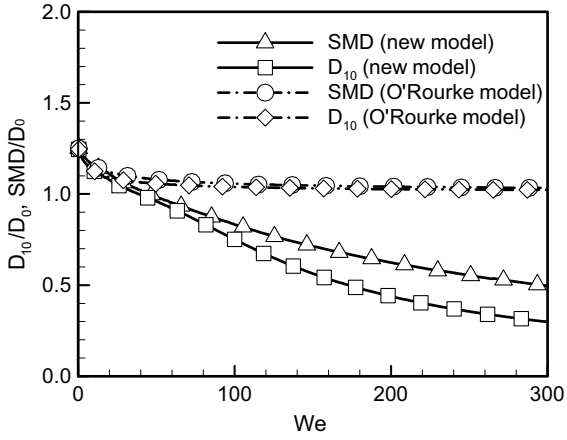

Fig. 11. Comparison between the predictions by both models for the D_{10} and SMD normalized by the initial droplet diameter D_0 for the binary collision of equal-sized water droplets.

these results, it is concluded that the new model is more reasonable than the O'Rourke model for simulation in the droplet collision process leading to the droplet breakup.

5. Conclusions

The present study has developed the new droplet collision model for consideration of the collision-induced breakup processes. In the new model, the post-collision characteristics of droplets were determined by the new formulae based on the conservation equations between before and after collision. For the validation of the new model, the calculated results are first compared with

experimental data (Ashgriz and Poo, 1990; Brenn et al., 2001) on the binary droplet collision. In the stretching separation regime, the number of satellite droplets is of the highest value in the range from 0.4 to 0.6 in impact parameter. In the reflexive separation regime, in addition, the satellite droplets are formed most actively in the case of the head-on collision. The predicted mean diameter by the new model decreased with increasing the Weber number because of the collision-induced breakup. The O'Rourke model, on the other hand, failed to predict the size reduction via the binary droplet collision. From these results, it can be concluded that the new model for droplet collision is more reasonable than the O'Rourke model for simulation in the collision-induced breakup process accompanied with formation of satellite droplets.

References

Arai, M., Saito, M., 1999. Atomization characteristics of jet-to-jet and spray-to-spray impingement systems. Atomization and Sprays 9, 399–417.

Ashgriz, N., Poo, J.Y., 1990. Coalescence and separation in binary collisions of liquid drops. J. Fluid Mech. 221, 183–204.

Bai, C., 1996. Modeling of spray impingement processes. Ph.D. Thesis, Imperial College of Science and Technology and Medicine, Department of Mechanical Engineering, University of London.

Brazier-Smith, P.R., Jennings, S.G., Latham, J., 1972. The interaction of falling water droplets: coalescence. Proc. Roy. Soc. Lond. A 326, 393–408.

Brenn, G., Valkovska, D., Danov, K.D., 2001. The formation of satellite droplets by unstable binary drop collisions. Phys. Fluids 13, 2463–2477.

Jiang, Y.J., Umemura, A., Law, C.K., 1992. An experimental investigation on the collision behavior of hydrocarbon droplets. J. Fluid Mech. 234, 171–190.

Ko, G.H., Lee, S.H., Ryou, H.S., Choi, Y.K., 2003. Development and assessment of a hybrid droplet collision model for two impinging sprays. Atomization and Sprays 13, 251–272.

O'Rourke, P.J., 1981, Collective drop effects on vaporizing liquid sprays, Ph.D. Thesis, Mechanical and Aerospace Engineering, Princeton University, USA.

O'Rourke, P.J., Bracco, F.V., 1980. Modeling of droplet interactions in thick sprays and a comparison with experiments. Proc. Inst. Mech. Eng. 9, 101–106.

Orme, M., 1997. Experiment on droplet collisions, bounce, coalescence and disruption. Progr. Energy Combust. Sci. 23, 65–79.

Post, S.L., Abraham, J., 2002. Modeling the outcome of drop–drop collisions in diesel sprays. Int. J. Multiphase Flow 28, 997–1019.

Qian, J., Law, C.K., 1997. Regimes of coalescence and separation in droplet collision. J. Fluid Mech. 331, 59–80.